

## Effect of Dibromothymoquinone on Chlorophyll *a* Fluorescence in *Chlamydomonas reinhardtii* Cells Incubated in Complete or Sulfur-Depleted Medium

A. A. Volgusheva, G. P. Kukarskikh, T. K. Antal, O. G. Lavrukhina,  
T. E. Krendeleva, and A. B. Rubin

Faculty of Biology, Moscow State University, Moscow, 119991 Russia

Received March 20, 2008

**Abstract**—The effect of dibromothymoquinone on chlorophyll fluorescence was studied in *Chlamydomonas reinhardtii* cells using PAM and PEA fluorometers. Dibromothymoquinone was shown to affect differently control cells incubated in complete medium and S-starved cells. The fluorescence yield in the control suspension considerably increased in the presence of the inhibitor. Presumably, this can be due to inactivation of protein kinase, as a result of which part of light-harvesting complex II that could have diffused from the stacking zone of the membrane into the lamellar zone towards photosystem I remains close to photosystem II. In S-starved cells, whose photosynthetic apparatus is in state 2, the fluorescence level declines in the presence of dibromothymoquinone. The JIP testing of induction curves (O-J-I-P fluorescence transient) suggests that dibromothymoquinone inhibits both light-harvesting complex II kinase and photosynthetic electron transport when added to the control, while in the starved cells it acts predominantly as an electron acceptor.

**Key words:** *Chlamydomonas reinhardtii*, dibromothymoquinone, sulfur deprivation, chlorophyll fluorescence.

**DOI:** 10.1134/S0006350908050102

### INTRODUCTION

When cultured on sulfur-free medium in closed bioreactors, algae *Chlamydomonas reinhardtii* produce hydrogen in the light. This phenomenon could be used as a biotechnological technique for time separation of the processes of oxygen and hydrogen production. The main donor of electrons for the hydrogenase reaction in these algae is water, but oxygen, which is evolved in the primary processes of photosynthesis, inhibits hydrogenase. When the medium is deficient in sulfur, the activity of photosystem (PS) II gradually decreases; the rate of oxygen evolution becomes lower than the rate of its consumption in respiration; the culture enters the anaerobic state; and, when hydrogenase is activated, hydrogen evolution starts [1–4]. During the first three days of sulfur starvation, there is almost no change in the chlorophyll content and concentration of cells in a suspension of *C. reinhardtii*, although there are considerable disruptions in the primary processes of photosynthesis [5]. The distribution of absorbed light energy among various pathways of its dissipation was found to vary. Photochemical quenching decreases due to a disruption of electron transport since some part of reaction

centers are damaged both at the acceptor (the appearance of  $Q_B$ -nonreducing centers) and the donor side, which is indicated by the appearance of a K peak in the kinetics of increasing fluorescence and by slowing of its dark relaxation [4, 6]. Despite a considerable increase in the content of  $Q_B$ -nonreducing centers, the quinone pool is over-reduced due to the electrons from endogenous reductants accumulated in sulfur deprivation via the chain of chlororespiration. It is this pathway that is considered as an additional source of electrons for the part of hydrogen production in light that is not suppressed by diuron [7]. The disruption of electron transport between the photosystems is accompanied by a decline in nonphotochemical quenching mainly due to the  $\Delta$ pH-dependent component  $qE$  and malfunction of the violaxanthin cycle [8]. On the contrary, dissipation by emission increases, which is indicated by a drastic (by two to three times) increase in fluorescence yield  $F_0$  calculated per chlorophyll unit [5, 8]. The increase in  $F_m$  that we found in response to sulfur starvation could be related to disruption of the dissipative cycle involving cytochrome  $b_{559}$  [9]. It was shown earlier that, in the case of sulfur starvation, the processes of migration of light-harvesting complex II (LHC II) between photosystems, which are related to the activities of LHC II kinase and phosphatase, are also disrupted; the photosynthetic apparatus of starved cells is predominantly in state 2 [5]. Although the molecular

**Abbreviations:** PS, photosystem; LHC II, light-harvesting complex; ETC, electron transport chain; DBMIB, dibromothymoquinone (2,5-Dibromo-3-methyl-6-isopropyl-*p*-benzoquinone).

mechanism of activation of LHC II kinase is not completely clear, there is no doubt that conformational change of one of the subunits of the cytochrome complex, the iron–sulfur Rieske protein, which is capable of changing its position in the membrane on reduction, plays an important role [10, 11]. Activation of this kinase is dynamic and could be induced by interaction of the Rieske protein with the transmembrane segment of the enzyme. In this work, we used the chlorophyll fluorometry technique, which allows one to monitor changes both in processes of photosynthetic electron transport and in transitions between states 1 and 2, and also provides information on the effects of dibromothymoquinone (DBMIB) on these two processes. This inhibitor was first introduced by Trebst [12, 13] as a specific inhibitor of the electron transport chain (ETC) at the level of the cytochrome complex. It competitively binds with the  $Q_o$  site, and it is important that complexes such as  $b_6/c$  are not sensitive to this inhibitor. Tightly bound with the cytochrome  $b_6/f$  complex, DBMIB prevents oxidation of PQH<sub>2</sub> molecules by the cytochrome complex [11, 14] and suppresses both electron transport and photoinduced hydrogen production [7]. During the process of binding of DBMIB at the  $Q_o$  site, the conformation of the Rieske subunit is fixed, preventing dynamic activation of LHC II kinase [15]. It is also demonstrated that in some cases it can accept electrons from  $Q_A^-$  [16]. Since sulfur-starved cells of *C. reinhardtii* differ from control cells in the state of the photosynthetic apparatus in respect to both energy coupling of antennas with reaction centers and the functioning of ETCs proper, it was of interest to compare the effects of DBMIB on the parameters of fluorescence in the control and sulfur-starved cultures.

## MATERIALS AND METHODS

**Cultivation of algae.** *C. reinhardtii* were grown photoheterotrophically in Tris–acetate–phosphate medium, pH 7.0, in 300-ml conical flasks on a shaker at 25°C and an illuminance of 100  $\mu\text{E m}^{-2} \text{s}^{-1}$  until they reached a concentration of  $(4\text{--}6) \times 10^6$  cells/ml (late logarithmic growth phase). Then cells were pelleted and resuspended three times in either sulfur-free medium or complete medium (control) and then incubated under similar conditions for 72 h. For cell cultivation of the D1-R323D mutant of *C. reinhardtii*, the illuminance was reduced to 50  $\mu\text{E m}^{-2} \text{s}^{-1}$ .

**PAM fluorometry.** Chlorophyll fluorescence was recorded using a PAM-2000 (pulse amplitude modulation) fluorometer (Walz, Germany); excitation was performed with 3- $\mu\text{s}$  modulated light pulses ( $0.1 \mu\text{E m}^{-2} \text{s}^{-1}$ ) fired at frequencies of 600 Hz in the dark and 20 kHz in the light (Stanley H-3000 light-emitting diodes,  $\lambda = 655 \text{ nm}$ ). Parameters of chlorophyll fluorescence were recorded using the Da-2000 computer program (Heinz, Walz). In our experiments, we measured the following

fluorescence parameters:  $F_0$ , chlorophyll fluorescence in dark-adapted samples;  $F_m$ , chlorophyll fluorescence in response to a 0.8-s saturating light flash, which reduces primary quinone acceptors  $Q_A$  to  $Q_A^-$  (20-W halogen lamp,  $\lambda < 710 \text{ nm}$ ,  $1100 \mu\text{E m}^{-2} \text{s}^{-1}$ ). Time courses of light induction and dark relaxation of variable fluorescence were recorded using the Run 6 standard program. The intensity of probing light was  $0.3 \mu\text{E m}^{-2} \text{s}^{-1}$ , the intensity of actinic light was  $450 \mu\text{E m}^{-2} \text{s}^{-1}$  (fired with a frequency of 20 kHz), and the period of illumination was 2 s.

**PEA fluorometry.** Time-resolved kinetics of fluorescence induction were recorded with a PEA (plant efficiency analyzer) fluorometer (Hansatech, United Kingdom). Chlorophyll fluorescence was excited with red light ( $\lambda = 650 \text{ nm}$ ) with an intensity of  $3000 \mu\text{E m}^{-2} \text{s}^{-1}$ . Fluorescence was recorded in the region  $>680 \text{ nm}$  with a time resolution of 10  $\mu\text{s}$  during the first 2 ms, 1 ms in the interval from 2 ms to 1 s, and 100 ms in the time interval starting from 1 s. The value of  $F_0$  was set as the fluorescence recorded 50  $\mu\text{s}$  after the onset of continuous illumination. A logarithmic time scale allowed resolution of the stages of fluorescence growth.

The concentration of cells used in our experiments was  $(5\text{--}6) \times 10^6$  cells/ml. Before measurement, samples were dark adapted for 3 min in the presence of an alcohol solution of DBMIB or the same concentration of alcohol (not exceeding 1%) in the control samples.

Quantitative analysis of the characteristics of primary processes of photosynthesis as revealed by the parameters of the kinetic curve was performed using the so-called JIP test, based on the theory of energy fluxes [17]. According to this theory, excitation energy in an antenna can be used for photosynthesis or dissipate in heat or fluorescence. The measured parameters of fluorescence and the equations used in the JIP test, as well as a short description of them, are presented in Table 1 [18].

## RESULTS AND DISCUSSION

The photosynthetic apparatus of higher plants and green algae can be in two states: high-fluorescence state 1, when most of LHC II is located near PS II, and low-fluorescence state 2, when a part of LHC II, phosphorylated by LHC II kinase, migrates to PS I [19]. The transition to state 2 can be experimentally induced without light, changing the redox state of the quinone pool [15]. Thus, when a suspension of *C. reinhardtii* microalgae is bubbled with argon, electron transporters between the photosystems are reduced, which triggers a transition to low-fluorescence state 2. Further illumination of the suspension in the presence of diuron leads to oxidation of the quinone pool due to activity of PS I and returns the photosynthetic apparatus to state 1. Such changes in the fluorescence level in control cells are reported in [5]. In sulfur-starved cells of *C. reinhardtii* illuminated

**Table 1.** Fluorescence parameters, equations used for calculation of JIP test parameters from these parameters, and explanations

Measured fluorescence parameters	
$F_0, F_{300\ \mu\text{s}}, F_J, F_I, F_{6\ \text{s}}$	Fluorescence yield after 50 $\mu\text{s}$ , 300 $\mu\text{s}$ , 2 ms, 20 ms, and 6 s after the onset of illumination
$F_p (= F_m)$	Maximum fluorescence yield
Area	Area under the fluorescence kinetic curve O-J-I-P and $F_m$ level
Parameters of JIP test	
$F_v = F_m - F_0$	Maximum variable fluorescence
$V_J = (F_J - F_0)/F_v$	Relative amplitude of O-J phase
$V_I = (F_I - F_J)/F_v$	Relative amplitude of J-I phase
$M_O = 4(F_{300\ \mu\text{s}} - F_0)/F_v$	Initial slope of O-J phase of fluorescence growth
$S_M = (\text{Area})/F_v$	Area under the fluorescence kinetic curve O-J-I-P and $F_m$ level, normalized by $F_v$
$ET_O/TR_O = (1 - V_J)$	Probability of electron transfer from $Q_A^-$ into quinone pool
$ET_O/ABS = (1 - (F_0/F_m)(1 - V_J))$	Quantum yield of electron transport ( $t = 0$ )
$q_E = (F_m - F_{6\ \text{s}})F_v$	Capacity for pH-induced non-photochemical quenching of fluorescence

in the presence of diuron, the fluorescence remains almost unchanged, which led us to conclude that their photosynthetic apparatus is predominantly in state 2. Data obtained in this work using DBMIB, which inhibits LHC II protein kinase, support this hypothesis. Figure 1 shows the effect of  $10^{-5}$  M DBMIB on changes in

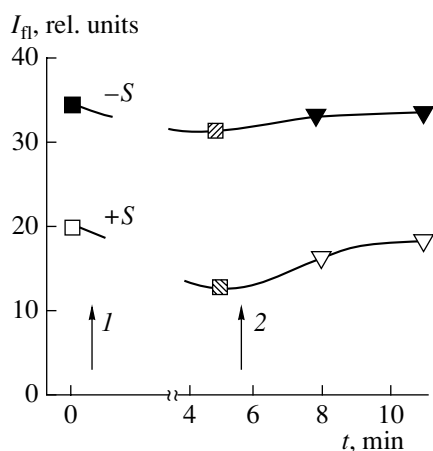


**Fig. 1.** Changes in chlorophyll fluorescence yield ( $I_{\pi}$ , rel. units) caused by transitions between states 1 and 2 in control (+S) and sulfur-starved (-S) for 48 h *C. reinhardtii* cells. Arrow 1 denotes argon bubbling of algae suspension; arrow 2 indicates introduction of  $10^{-5}$  M DBMIB.

chlorophyll fluorescence yield induced by redistribution of LHC II between PS II and PS I in the control (+S) and sulfur-starved (-S) cells of *C. reinhardtii*. Figure 1 shows that addition of the inhibitor to a suspension of algae brought into state 2 by argon bubbling increased the fluorescence of control cells (+S) and had almost no effect on the fluorescence of sulfur-starved (-S) cells. Unlike in the control cells, DBMIB does not switch the photosynthetic apparatus from state 2 to state 1 in sulfur-starved cells. The results presented below demonstrate that DBMIB had a different effect on the other parameters of fluorescence in control and sulfur-starved cells.

Figure 2 shows changes in the fluorescence parameters  $F_0$  and  $F_m$  normalized by chlorophyll concentration in the control (+S) and sulfur-starved (-S) cell suspensions with  $10^{-5}$  M DBMIB. It can be seen that introduction of DBMIB into the control suspension increased both  $F_0$  and  $F_m$ , the change in  $F_m$  being considerably greater than that in  $F_0$ . An increase in the  $F_0$  level is usually attributed to changes in antenna-reaction center interaction due to partial dissociation of low-molecular-weight antennas or damage of the structure of complexes; as a result, part of the excitation energy is lost as fluorescence during its migration in the pigment matrix [20]. The increase in the  $F_0$  level in the presence of diuron is explained by return of an electron from  $Q_B$  to  $Q_A$  when the inhibitor is bound with  $Q_B$  [21]. Presumably, DBMIB affects  $F_0$  by the same mechanism because there is a possibility of interaction of DBMIB with  $Q_B$  [16, 22]. We suggest that the considerable increase in the  $F_m$  level is related to the effect of DBMIB on LHC II kinase. In the control cells, LHC II can be bound not only with PS II; some part of it can also be associated with PS I, which lowers the apparent  $F_m$  level. In the presence of DBMIB, LHC II could not be phosphorylated and move towards PS I; as a result, the absorption cross section of PS II in the presence of the inhibitor is larger than without it, and consequently  $F_m$  becomes greater (Fig. 2a). In sulfur-starved *C. reinhardtii*, both  $F_0$  and  $F_m$  increase with starvation. Using pico- and nanosecond fluorometry, we demonstrated that the increase in fluorescence in starved cells results from disruption of the processes of electron transport and the appearance of long-lived states of  $Q_A^-$  [23]. As in the control cells, addition of  $10^{-5}$  M DBMIB to cells after first 24 h of starvation increased  $F_0$  and considerably increased  $F_m$ . After 48 h of starvation, the inhibitor had almost no effect on the fluorescence parameters. Unlike in the control cells, the  $F_m$  level in the presence of DBMIB even declined during further starvation (Fig. 2b). This is even more obvious from the time courses of fluorescence recorded by the PAM technique (Fig. 3). Several components could be distinguished in the time course of fluorescence in the light: an initial fast component ( $F_0 - F_I$ ), which is determined by the presence

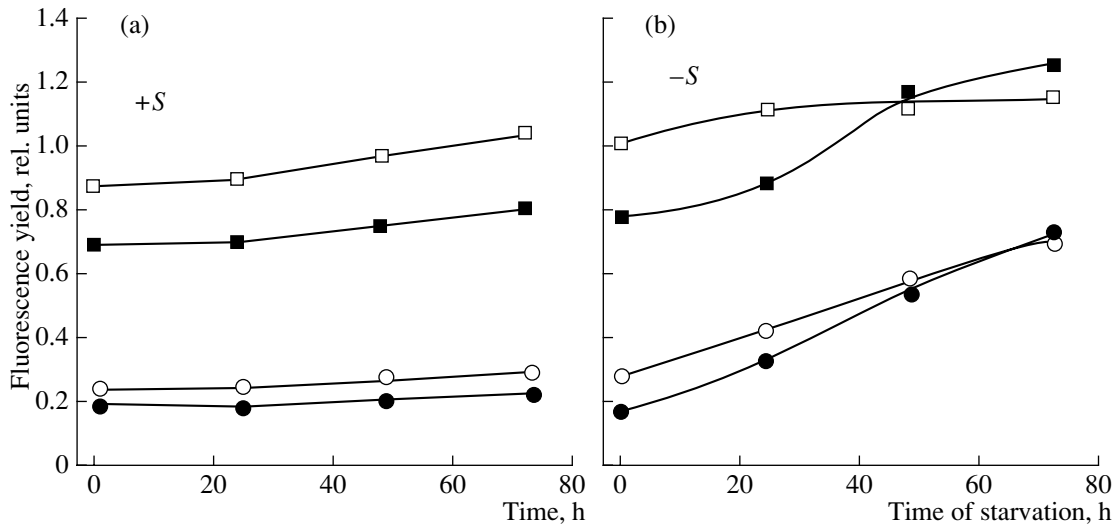


**Fig. 2.** Effect of  $10^{-5}$  M DBMIB on fluorescence parameters  $F_0$  (circles) and  $F_m$  (squares) in control (a) and sulfur-starved (b) cells of *C. reinhardtii* recorded by PAM fluorometry (filled circles and squares, without inhibitor; empty circles and squares, in the presence of the inhibitor).

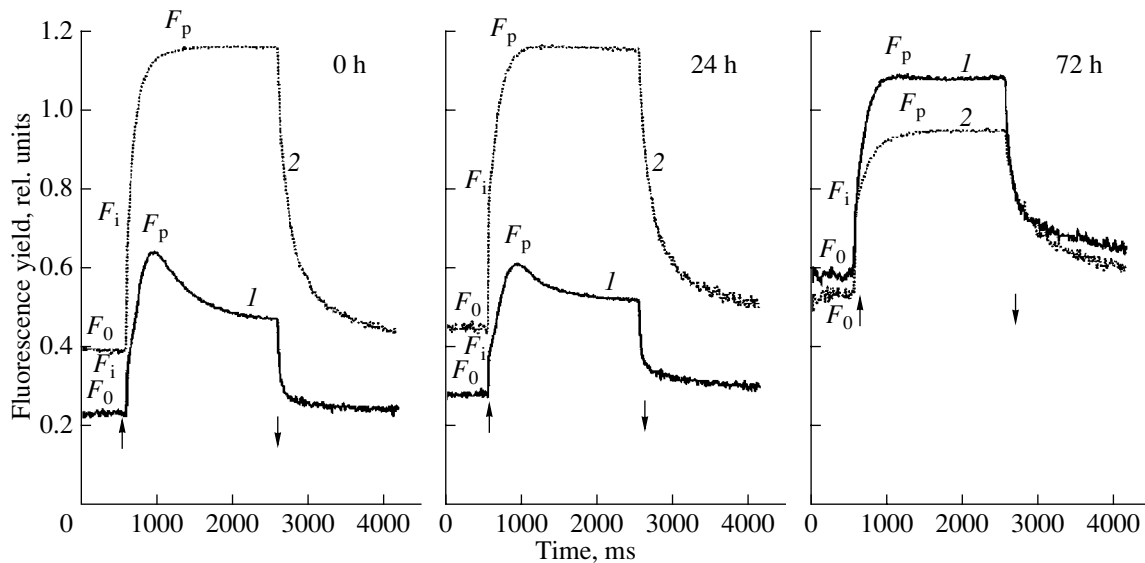


**Fig. 3.** Effect of DBMIB on fluorescence time course in control (0 h) and sulfur-starved (24 and 72 h of starvation) cells of *C. reinhardtii* recorded by the PAM technique: (1) without inhibitor; (2)  $10^{-5}$  M DBMIB. The upward arrow indicates the onset of actinic light ( $450 \mu\text{E m}^{-2} \text{s}^{-1}$ ); the downward arrow denotes switching off of the light.

of  $Q_B$ -nonreducing centers in PS II, and a slow component ( $F_i - F_p$ ), determined by the presence of  $Q_B$ -reducing centers. After the maximum fluorescence level is reached ( $F_p = F_m$ ), it declines in the light, which is believed to be related to oxidation of the quinone pool by PS I and development of nonphotochemical quenching [24]. Addition of DBMIB (Fig. 3, curves 2) to the control suspension (0 h) considerably changed the induction curve: fluorescence growth became faster, but still with two phases, and the  $F_0$  level increased slightly, the value of  $F_0 - F_i$  increased considerably, and

the  $F_p$  level rose drastically. Addition of  $10^{-5}$  M DBMIB almost doubled the maximum fluorescence level  $F_p$ . In the presence of DBMIB, the fluorescence level did not decline after the maximum value  $F_p$ . Figure 3 also indicates that, compared to the control cells,  $F_0$  and  $F_p$  levels increased as the starvation of *C. reinhardtii* proceeded. In addition, we observed a gradual decrease in the fluorescence decline after the peak  $F_p$  was reached up to complete disappearance of such a decline by 72 h (Fig. 3, curve 1). This is typically related to an increase in the degree of reduction on the

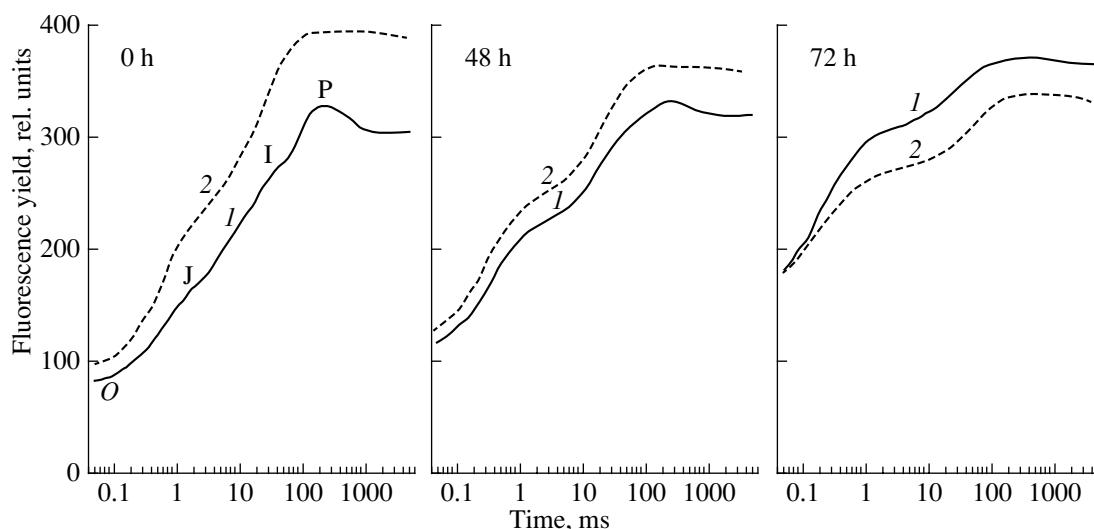


**Fig. 4.** Effect of DBMIB on fluorescence induction curves in control (0 h) and sulfur-starved (48 and 72 h of starvation) cells of *C. reinhardtii* recorded by the PEA method. The O-J-I-P transitions were induced by light with an illuminance of  $3000 \mu\text{E m}^{-2} \text{s}^{-1}$ : (1) without inhibitor; (2)  $10^{-6}$  M DBMIB.

acceptor side of PS I and a decline in the processes of nonphotochemical quenching [8]. Figure 3 shows that, at the beginning of starvation (24 h), DBMIB had an effect similar to that in the control cells. As the starvation proceeded, the increase in  $F_0$  and  $F_p$  levels in DBMIB-treated cells became smaller, so that by 72 h of starvation in the presence of DBMIB the value of variable fluorescence ( $F_p - F_0$ ) became even lower than that without the inhibitor (72 h, Fig. 3, curve 2).

DBMIB, a quinone, in the oxidized state can be a quencher of fluorescence according to the Stern-Volmer equation if the concentration of the inhibitor is high enough [22, 25]. To avoid a quenching effect, we lowered the DBMIB concentration to  $10^{-6}$  M and used a PEA fluorometer to obtain time-resolved fluorescence induction curves. The time course of chlorophyll fluorescence induction by intense light has several components, so-called O-J-I-P transitions. They are related to a gradual decline in photochemical quenching and the development of nonphotochemical quenching of fluorescence in PS II [26]. The O-J phase is due to light-induced single reduction of  $Q_A$ , whereas the J-I and I-P phases reflect mainly further accumulation of reduced  $Q_A^-$  caused by slowing of its reoxidation due to reduction of  $Q_B$  and the quinone pool. The O and P levels in the time course correspond to the  $F_0$  and  $F_m$  values [18]. Figure 4 shows fluorescence induction curves in the control and sulfur-starved cells of *C. reinhardtii* (normalized by chlorophyll) obtained under illumination with continuous light with an illuminance of  $3000 \mu\text{E m}^{-2} \text{s}^{-1}$ . All three phases (O-J, J-I, and I-P) and the decline in the fluorescence level after the maximum value is reached (0 h, Fig. 4, curve 1) are clearly distinct in the fluorescence time course in the control culture. As was noted

earlier, we observed an increase in the  $F_0$  (O) and  $F_m$  (P) levels and a considerable change in the shape of the curve in the starved culture compared to the control culture, which became even greater as the starvation proceeded. Thus, we observed a considerable increase in the growth rate of the O-J phase and a decrease in the O-P amplitude and the contribution of the J-I-P phase in the fluorescence time course of the sulfur-starved cells. In addition, we did not find a distinct transition between the J-I and I-P phases [6]. Addition of  $10^{-6}$  M DBMIB to the control suspension somewhat increased  $F_0$  (O), decreased the time required to reach P, and considerably increased the maximum level of P. In the presence of the inhibitor, the decline in fluorescence level after reaching P (0 h, Fig. 4, curve 2) disappeared. In the case of the sulfur-starved culture, in the first hours of starvation the DBMIB-induced increase in the P level was smaller than in the control culture. After 48 h of starvation, the P level did not increase, whereas in the case of longer starvation the P level in the presence of the inhibitor was lower than without it (48 and 72 h, Fig. 4, curves 2).

To understand why the effect of DBMIB on control and starved cells is different, we performed a quantitative analysis of the characteristics of primary photosynthetic processes by kinetic parameters, employing the so-called JIP test, based on the theory of energy fluxes [17]. Table 2 shows the obtained parameters of the JIP test for control and sulfur-starved cells of *C. reinhardtii* in the absence and the presence of DBMIB. The parameters were calculated by the equations presented in Table 1. The parameter  $M_0$  characterizes the initial slope of the O-J growth phase on the fluorescence time course. The increase in the parameter  $M_0$  in the starved cells indicates the appearance of  $Q_B$ -nonreducing cen-

**Table 2.** Measured fluorescence parameters and JIP test parameters calculated from the fluorescence kinetic curves O-J-I-P measured by the PEA method in control (0 h) and sulfur-starved cells of *C. reinhardtii* (48 and 72 h)

Parameters of JIP test	0 h	DBMIB (10 <sup>-6</sup> M)	48 h	DBMIB (10 <sup>-6</sup> M)	72 h	DBMIB (10 <sup>-6</sup> M)
$F_0$	82	98	118	130	183	181
	100%	119%	100%	110%	100%	99%
$F_p(=F_M)$	326	393	332	363	370	336
	100%	121%	100%	109%	100%	91%
$V_j$	0.34	0.43	0.48	0.50	0.65	0.56
	100%	127%	100%	104%	100%	86%
$M_O$	0.41	0.52	0.82	0.96	1.50	1.32
	100%	127%	100%	117%	100%	88%
$S_M$	0.36	0.18	0.20	0.13	0.09	0.15
	100%	50%	100%	65%	100%	166%
$ET_O/TR_O$	0.66	0.57	0.52	0.50	0.35	0.44
	100%	86%	100%	96%	100%	126%
$ET_O/ABS$	0.50	0.43	0.34	0.32	0.18	0.20
	100%	86%	100%	94%	100%	111%
$q_E$	0.10	0.02	0.06	0.02	0.04	0.05
	100%	20%	100%	33%	100%	125%

ters of PS II, incapable of reducing the quinone pool. This conclusion is also supported by an increase in the time required to reach P by more than one and a half times by 72 h of starvation and a decrease in the parameters  $ET_O/ABS$  and  $S_M$ , which characterize the quantum yield and the rate of electron transport, respectively. The more than double decrease in the value of the parameter  $q_E$  indicates a decline in capacity for  $\Delta pH$ -induced nonphotochemical quenching of fluorescence. Table 2 suggests that DBMIB treatment induced a 20% increase in the  $F_0$  level in control samples. In the sulfur-starved cells, the  $F_0$  level in the presence of DBMIB remained almost the same. The maximum fluorescence yield  $F_p$  in control cells treated with DBMIB also increased by 20%. On the contrary, DBMIB treatment of the long-starved cells slightly decreased the  $F_p$  level. Introduction of 10<sup>-6</sup> M DBMIB into the suspension of control cells increased the  $M_O$  value by almost 30%, whereas, in the starved cells, the value of this parameter slightly decreased (by 12% by 72 h of starvation). These data agree well with the results obtained for the parameter  $V_j$ , which reflects the relative amplitude of the O-J phase. This parameter increased in the control cells treated with the inhibitor and decreased in the starved cells. In the control cells treated with DBMIB, the value of  $S_M$  (the area under the curve normalized by  $F_p$ ) decreased by half, which suggests a reduction of electron flow from PS II into the quinone pool. In the starved cells (in which  $S_M$  is lower than in the control cells), DBMIB increased the  $S_M$  value by more than 40% by 72 h of starvation. The parameter  $ET_O/TR_O$ ,

which characterizes the probability of electron transfer from  $Q_A^-$  further in the ETC, behaved similarly. Table 2 shows that in control cells DBMIB treatment decreased  $ET_O/TR_O$  by almost 15%, whereas, in the starved cells (by 72 h of starvation), the value of this parameter increased by almost a third. This is also in agreement with DBMIB-induced changes in  $ET_O/ABS$  (the quantum yield of electron transport at  $t = 0$ ): it decreased by 14% in the control cells and somewhat increased in the long-starved cells. In control cells, DBMIB lowered the parameter  $q_E$ , which reflects the capacity for  $\Delta pH$ -induced nonphotochemical quenching of fluorescence, by 80%, which could be related to a decrease in the number of functioning ETCs. In the starved cells, where this parameter was considerably lower, addition of DBMIB increased the  $q_E$  value by more than 20% by 72 h of starvation, presumably due to stimulation of electron flow.

Thus, the data obtained in this work suggest that DBMIB has a different effect on fluorescence of normal and sulfur-starved cells of *C. reinhardtii*. Addition of DBMIB to a suspension of control cells decreases all the parameters related to the activity of ETCs. According to the conventional view, DBMIB binds to the  $Q_o$  site of the cytochrome complex, disrupting linear electron transport, which leads to an increase in reduction of the quinone pool. This could explain the increase in the amplitude of the O-J phase of the time course and acceleration of fluorescence growth  $M_O$ . However, this could not explain such a considerable increase in the maximum fluorescence level in the control cell suspen-

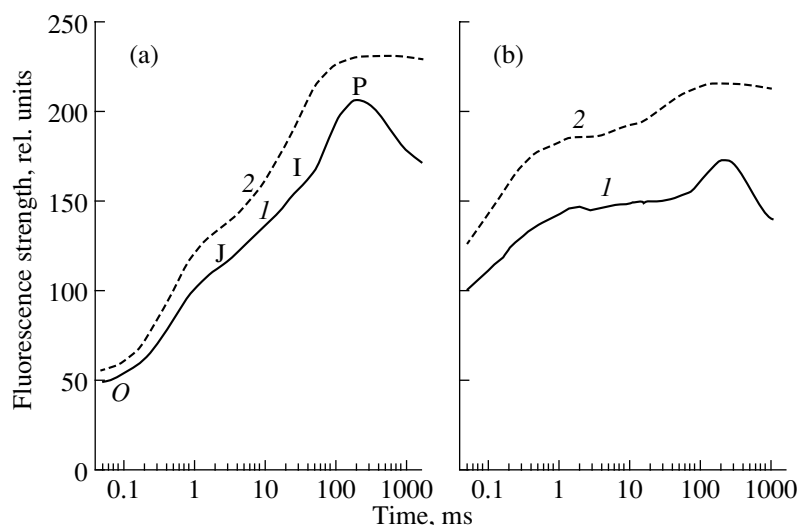


**Fig. 5.** Effect of DBMIB on the fluorescence induction curves in pseudo-wild-type *C. reinhardtii* (a) and D1-R323D mutant (b) cells. The O-J-I-P transitions were induced by light with an illuminance of  $3000 \mu\text{E m}^{-2} \text{s}^{-1}$ : (1) without inhibitor; (2)  $10^{-6}$  M DBMIB.

sions treated with the inhibitor (Figs. 3, 4). As was shown earlier, in higher plants, DBMIB accelerates fluorescence growth and prevents its decay after the maximum level P is reached, but does not exceed the level of maximum fluorescence [16, 22]. It is also known that in higher plants only about 20% of LHC II can migrate from PS II to PS I during the transition from state 1 to state 2, whereas in green microalgae this proportion is about 85% [27, 28]; therefore, considerable changes in the fluorescence level can be expected in microalgae. In connection with this, we suggest that the increase in the level of maximum fluorescence in control suspensions treated with DBMIB could be related to suppression of protein kinase activity, as a result of which part of LHC II, which could have drifted from the stacking zone of the membrane into the lamellar zone towards PS I, remains associated with PS II, thus ensuring a high-fluorescence state. If in sulfur-starved cells the photosynthetic apparatus is continually in state 2, the suppression of LHC II kinase by DBMIB cannot elevate the fluorescence level, which we observed in our experiments. Furthermore, with long-term starvation, we found a decline in the fluorescence level and a decrease in  $M_0$  and  $V_j$  in the presence of DBMIB (Figs. 3, 4), which suggests, on the contrary, acceleration of electron flow. We believe that DBMIB in chloroplasts of long-starved cells, in contrast to control cells, can accept electrons from ETCs. It is known that, under some conditions, reduced DBMIB can donate electrons to plastocyanin and  $\text{P700}^+$ , whereas molecules of oxidized DBMIB, when bound to  $\text{Q}_B$ , accept electrons from  $\text{Q}_A^-$ , thus shunting the chain [16]. This hypothesis is supported by the data on other parameters of the JIP test that characterize electron transport ( $ET_0/ABS$ ,  $ET_0/TR_0$ ,  $q_E$ ). Presumably, in sulfur starvation, in which synthesis (and, consequently,

renewal of proteins) is limited [29], such structural damage to membranes takes place in the chloroplasts, which affects the interaction of DBMIB with components of ETCs between the photosystems.

The D1-R323D mutant of *C. reinhardtii* was provided to us by staff of the Department of Plant Biology, Ohio State University (United States). This mutation disrupts the interaction of the oxygen-evolving complex with the reaction center. However, since this is a point mutation, changing a single amino acid in the D1 protein, the structure of the other membrane components presumably remains intact, in contrast to the situation with sulfur-starved cells. As revealed by EPR spectroscopy, even the PS II complex is fully formed in this mutant [31]. Functional damage of ETCs in this mutant and in wild-type cells of *C. reinhardtii* grown under sulfur-starvation conditions is similar (damage on the donor side of PS II, accumulation of  $\text{Q}_B^-$ -nonreducing centers) [30, 31]. The fluorescence induction curve in the mutant is also similar to the induction curve in sulfur-starved cells: a high  $F_0$  level, the presence of a K peak, the absence of a clearly distinct J-I phase (Fig. 5b, curve 1). However, the effect of DBMIB on the D1-R323D mutant grown on complete nutrient medium was similar to its effect on wild-type cells. Figure 5 (curve 2) shows that  $10^{-6}$  M DBMIB increased the P level in both mutant and wild-type cells. We suggest that this increase in the maximum fluorescence in both samples is related to inhibition of LHC II kinase. Unlike in the sulfur-starved cells, the structure of protein components of ETCs between the photosystems in the mutant is not changed; therefore, no effect of DBMIB as an acceptor was found.

## ACKNOWLEDGMENTS

This work was supported by the Russian Foundation for Basic Research, project nos. 07-04-00222 and 08-04-90205.

## REFERENCES

1. A. Melis, L. Zhang, M. Forestier, et al., *Plant Physiol.* **122**, 127 (2000).
2. T. K. Antal, T. E. Krendeleva, T. V. Laurinavichene, et al., *Dokl. Akad. Nauk* **381** (1), 119 (2001) [*Dokl. Biochem. Biophys.* **381** (1), 371–375 (2001)].
3. S. Kosourov, A. Tsygankov, M. Seibert, and M. L. Ghirardi, *Biotechnology and Bioengineering* **78** (7), 731 (2002).
4. T. K. Antal, T. E. Krendeleva, T. V. Laurinavichene, et al., *Biochim. Biophys. Acta* **1607**, 153 (2003).
5. T. K. Antal, A. A. Volgusheva, G. P. Kukarskikh, et al., *Biofizika* **51** (2), 292 (2006) [*Biophysics* **51** (2), 251–257 (2006)].
6. T. K. Antal, T. E. Krendeleva, and A. B. Rubin, *Photosynth. Res.* **94**, 13 (2007).
7. S. Kosourov, M. Seibert, and M. L. Ghirardi, *Plant Cell. Physiol.* **44** (2), 146 (2003).
8. T. K. Antal, A. A. Volgusheva, G. P. Kukarskikh et al., *Physiol. Plant.* **128**, 128 (2006).
9. D. Lazar, P. Ilic, J. Kruk, et al., *J. Theoretical Biology* **233**, 287 (2005).
10. F. Zito, G. Finazzi, R. Delosme, et al., *EMBO J.* **18**, 2961 (1999).
11. A. V. Vener, I. Ohad, and B. Andersson, *Current Opinion in Plant Biol.* **1**, 217 (1998).
12. A. Trebst, E. Harth, and W. Draber, *Z. Naturforsch.* **25b**, 1157 (1970).
13. H. Böhme, S. Reimer, and A. Trebst, *Z. Naturforsch.* **26b**, 341 (1971).
14. P. R. Rich, S. A. Madwick and D. A. Moss, *Biochim. Biophys. Acta* **1058**, 312 (1991).
15. G. Finazzi, F. Zito, R. P. Babagallo, and F. A. Wollman, *J. Biol. Chem.* **276** (13), 9770 (2001).
16. G. Schansker, S. Z. Toth and R. J. Strasser, *Biochim. Biophys. Acta* **1706**, 250 (2005).
17. B. J. Strasser and R. J. Strasser, in *Photosynthesis: from Light to Biosphere*, Ed. by P. Mathis (Kluwer, Dordrecht, 1995), vol. 4, pp. 909–912.
18. R. J. Strasser, M. Tsimilli-Michael, and A. Srivastava, in *Chlorophyll a fluorescence: A Signature of Photosynthesis. Advances in Photosynthesis and Respiration*, Ed. by G. C. Papageorgiou and Govindjee (Springer, Dordrecht, 2004) vol. 19, pp. 321–362.
19. J. F. Allen, J. Bennet, K. E. Steinback, and C. J. Arntzen, *Nature* **291**, 25 (1981).
20. J.-M. Briantais, J. Dacosta, Y. Goulas., et al., *Photosynth. Res.* **48**, 189 (1996)
21. M. Hiraki, J. J. S. van Rensen, W. J. Vredenberg and K. Wakabayashi, *Photosynth. Res.* **78**, 35 (2003).
22. N. G. Bukhov, G. Sridharan, E. A. Egorova, and R. Carpentier, *Biochim. Biophys. Acta* **1604**, 115 (2003).
23. A. Volgusheva, V. E. Zagidullin, T. K. Antal et al., *Biochim. Biophys. Acta* **1767**, 559 (2007).
24. D. Lazar, *Biochim. Biophys. Acta* **1412**, 1 (1999).
25. K. K. Karukstis, *J. Photochem. Photobiol., B* **15**, 63 (1992).
26. D. Lazar, *Funct. Plant Biol.* **33**, 9 (2006).
27. G. Finazzi, *J. Exp. Botany* **56**, 383 (2005).
28. N. G. Bukhov, *Fiziologiya Rastenii* **51** (6), 825 (2004) [*Russ. J. Plant Physiol.* **51** (6), 742–753 (2004)].
29. L. Zhang, H. Happe, and A. Melis, *Planta* **214**, 552 (2002).
30. V. V. Makarova, S. N. Kosourov, T. E. Krendeleva, et al., *Biofizika* **50** (6), 1070 (2005) [*Biophysics* **50** (6), 1070 (2005)].
31. V. V. Makarova, S. Kosourov, T. E. Krendeleva, et al., *Photosynth. Res.* **94**, 79 (2007).